Available online at www.sciencedirect.com
ScienceDirect
Scripta Materialia xxx (2008) xxx–xxx
Scripta MATERIALIA
www.elsevier.com/locate/scriptamat

On the negative strain rate sensitivity of Hadfield steel

D. Canadinc,[a,*] C. Efstathiou[b] and H. Sehitoglu[b]

[a] *Koc University, Department of Mechanical Engineering, Sariyer 34450 Istanbul, Turkey*
[b] *University of Illinois at Urbana-Champaign, Department of Mechanical Science and Engineering, Urbana, IL 61801, USA*

Received 4 June 2008; revised 17 July 2008; accepted 18 July 2008

The room temperature strain rate sensitivity of Hadfield steel polycrystals was investigated with the aid of in situ digital image correlation. The current findings indicate that both the rapid work hardening and negative strain rate sensitivity of Hadfield steel polycrystals are influenced by dynamic strain aging.

Keywords: Hadfield steel; Strain hardening; Negative strain rate sensitivity; Dynamic strain aging; Digital image correlation

The digital image correlation (DIC) technique was utilized in conjunction with mechanical experiments carried out at different strain rates to study the negative strain rate sensitivity (NSRS) in face-centered cubic (fcc) Hadfield steels. The results shed light onto the variation of local strain fields and serrations in the stress–strain curves of Hadfield steels as a function of strain rate within the NSRS range.

Contradictory explanations regarding the main cause of rapid work hardening of Hadfield steel, such as twin boundaries, stacking faults and dynamic strain aging (DSA), warrant a detailed investigation of the proposed causes [1–14]. This particular study focuses on DSA and its role on the strain hardening behavior of Hadfield steel, and presents a new systematic set of results on the influence of DSA on the rapid work hardening in Hadfield steel.

Previously, DSA was investigated by means of classical thermo-mechanical experimentation techniques [1] and numerical models utilizing a statistical approach [3]. Specifically, DSA is brought about by the reorientation of carbon members of manganese–carbon (Mn–C) couples in the cores of dislocations. At elevated temperatures this reorientation of Mn–C couples is enhanced due to increased energy of the system, promoting the diffusivity of C atoms, eventually leading to rapid strain hardening in the absence of twin formation [1,3].

While there are a very limited number of studies focusing on the DSA in Hadfield steel, DSA and strain rate sensitivity (SRS) in metallic alloys have been the focus of attention in many works [15–22]. Numerical models were developed based on the theoretical framework; however, the analyses were mostly confined to the statistical evaluation of shear localization during deformation, and the Portevin Le Chatelier (PLC) effect. The current study approaches the problem of DSA and SRS in Hadfield steel from an experimental point of view, namely by adopting the DIC technique as an in situ aid to the classical uniaxial deformation experiments.

Advanced imaging techniques, such as DIC [23–30] and infrared imaging [31,32], have recently been successfully utilized in various studies investigating the deformation of metallic materials in order to monitor the formation and evolution of local strain fields. In the current work, DIC was used to associate the macroscopic effects of DSA with the corresponding theoretical considerations, which are impractical to monitor in an in situ fashion. Particularly, monitoring of the strain localization and the evolution of strain fields by DIC serves as indirect evidence of the microscopic mechanisms facilitating DSA.

The material investigated in this study is fcc Hadfield steel, with a chemical composition of 12.44 wt.% Mn, 1.10 wt.% C and balance iron (Fe). Small-scale dog-bone-shaped tension samples were extracted from railroad frogs taken from service utilizing electro-discharge machining. The monotonic tensile deformation experiments were carried out on a servo-hydraulic test frame

* Corresponding author. Tel.: +90 212 338 1891; fax: +90 212 338 1548; e-mail: dcanadinc@ku.edu.tr

1359-6462/$ - see front matter © 2008 Acta Materialia Inc. Published by Elsevier Ltd. All rights reserved.
doi:10.1016/j.scriptamat.2008.07.027

equipped with a digital controller and a miniature extensometer of 3 mm gauge length. The results revealed a significant SRS prevalent in Hadfield steel polycrystals within the strain rate ($\dot{\varepsilon}$) range of $1\cdot10^{-5}\frac{1}{s}<\dot{\varepsilon}<1\cdot10^{-1}\frac{1}{s}$ (Fig. 1). A serrated flow is evident at all strain rates; however, the associated instability is much more prominent within $1\cdot10^{-4}\frac{1}{s}<\dot{\varepsilon}<1\cdot10^{-2}\frac{1}{s}$, where the material exhibits NSRS. Normally, increased $\dot{\varepsilon}$ enhances dislocation density and results in additional strengthening, which is, for instance, evident as the $\dot{\varepsilon}$ is increased from $1\cdot10^{-5}\frac{1}{s}$ to $1\cdot10^{-4}\frac{1}{s}$ and from $1\cdot10^{-2}\frac{1}{s}$ to $1\cdot10^{-1}\frac{1}{s}$. On the contrary, an increase of $\dot{\varepsilon}$ from $1\cdot10^{-4}\frac{1}{s}$ to $1\cdot10^{-3}\frac{1}{s}$ and from $1\cdot10^{-3}\frac{1}{s}$ to $1\cdot10^{-2}\frac{1}{s}$ yields a softening in the overall deformation response, which is known as the NSRS [33].

Stress drops due to flow localization follow a periodic pattern, and the magnitude of the stress drops increases within the NSRS range (Fig. 1), demonstrating the increased instability brought about by the local softening of the material associated with the local increase in $\dot{\varepsilon}$. Strain rate jump experiments clearly demonstrate the NSRS of Hadfield steel (Fig. 2). An abrupt change in $\dot{\varepsilon}$ results in an instantaneous change in flow stress, $\Delta\sigma_i$, which is always positive [20], and this change in the deformation response is reflected by the instantaneous SRS, denoted by $M_i=\frac{d\sigma_i}{d\ln\dot{\varepsilon}}$. However, whether the SRS is negative or positive is based on the steady-state strain rate sensitivity, $M_s=\frac{d\sigma_{ss}}{d\ln\dot{\varepsilon}}$, which considers the difference in stable flow stress, $\Delta\sigma_{ss}$, following the strain rate jump [20,21]. In the NSRS regime, $\Delta\sigma_{ss}$ and M_s are negative, and become positive outside the NSRS regime. For instance, a strain rate jump from $1\cdot10^{-4}\frac{1}{s}$ to $1\cdot10^{-3}\frac{1}{s}$ at about 2% true inelastic strain yields $\Delta\sigma_{ss}=-11$ MPa, implying an NSRS, whereas a strain rate jump from $1\cdot10^{-2}\frac{1}{s}$ to $1\cdot10^{-1}\frac{1}{s}$ at about 7% true inelastic strain brings about $\Delta\sigma_{ss}=+27$ MPa, which is outside the NSRS range.

DSA is attributed to the pinning of mobile dislocations arrested at obstacles by the solute atoms diffusing within the matrix [17]. When dislocation glide is hindered by obstacles, there is an elapse of time before the dislocations overcome the obstacles. The average time the dislocations stay arrested at obstacles throughout the matrix is defined as the waiting time, t_w, which is proportional to the density of mobile dislocations (ρ_m), the dislocation mean free path (L) and the inverse of strain rate ($1/\dot{\varepsilon}$). The Orowan equation defines the waiting time as $t_w=\rho_m bL/\dot{\varepsilon}$ [17,20,21]. During the waiting time, solute atoms might diffuse into the arrested dislocations, leading to DSA [17]. One can picture the rapid strain hardening of Hadfield steel as a superposition of contributions from slip and DSA [1–14], yet the strain rate dictates the cooperation of these factors and the respective importance of their contributions to the overall hardening. Note that twin stress and the corresponding twin barriers to dislocation motion are not rate dependent [34], thus variation of the strain rate does not change the contribution of twinning to work hardening.

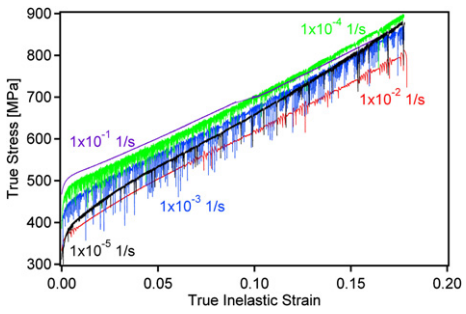

Figure 1. The room temperature strain rate dependence of the monotonic tensile deformation response of Hadfield steels. Each curve is representative of 3–5 experiments.

Specifically, as the $\dot{\varepsilon}$ increases, t_w decreases, leaving less time for C atoms to age the interrupted dislocations. Nevertheless, the increasing strain rate also increases the energy of the system, providing more energy to C atoms, eventually enhancing the ability of C to diffuse within the matrix and pin the arrested dislocations. Experimentally, the macroscopic effect of this competition between the diffusivity of C and the aging of blocked dislocations by C is observed in the form of an overall decrease in the strength levels, NSRS, and the accompanying instabilities (Figs. 1 and 2). The increased magnitude of (local) stress drops and the loss of strength despite the increasing $\dot{\varepsilon}$ within a range of $1\cdot10^{-4}\frac{1}{s}<\dot{\varepsilon}<1\cdot10^{-2}\frac{1}{s}$ clearly demonstrate the associated instability owing to the elevated state of energy in the system. Once the $\dot{\varepsilon}$ exceeds $1\cdot10^{-2}\frac{1}{s}$, the NSRS diminishes and a more stable deformation response with stress drops much smaller in magnitude is evident.

As DSA leads to local instabilities throughout the material, in situ DIC was utilized in order to closely monitor the evolution of the strain field in the gauge section of the samples. For DIC analysis, two strain rates were chosen within the range of NSRS, namely $1\cdot10^{-4}\frac{1}{s}$ and $1\cdot10^{-3}\frac{1}{s}$. The specimen surfaces were polished prior to testing, and a speckle pattern was spray painted onto them for referencing the images. In situ images were captured with cameras set at 1600×1200 and 1280×960 pixels. The image acquisition was programmed into the mechanical testing software, and the displacements were measured by tracking the evolution of the speckle pattern with deformation. Finally, a commercial software was utilized to correlate images and calculate strains from displacement gradients.

Based on the DIC results (Fig. 3), a non-uniform distribution of the strains within the gauge sections is evident at both strain rates. However, the degree of non-uniformity is relatively higher at $\dot{\varepsilon}=1\cdot10^{-3}\frac{1}{s}$ (Fig. 4), where the macroscopic deformation response exhibits larger stress drops, and a higher degree of local instability and associated local softening. The direct correlation between the uniformity of the strain fields and the instability of the tensile deformation curves is also noteworthy. For instance, at $\dot{\varepsilon}=1\cdot10^{-4}\frac{1}{s}$, the stress drops become quite small in magnitude at about 15% true inelastic strain, where the calculated strain field exhibits a mostly uniform distribution.

A comparison of strain localization at similar strains in Hadfield steel polycrystals deformed at $\dot{\varepsilon}=1\cdot10^{-4}\frac{1}{s}$ and $\dot{\varepsilon}=1\cdot10^{-3}\frac{1}{s}$ reveals that the latter strain rate brings about more variation in strain within the gauge section (Fig. 4). Furthermore, no evidence of PLC bands is

Please cite this article in press as: D. Canadinc et al., Scripta Mater. (2008), doi:10.1016/j.scriptamat.2008.07.027

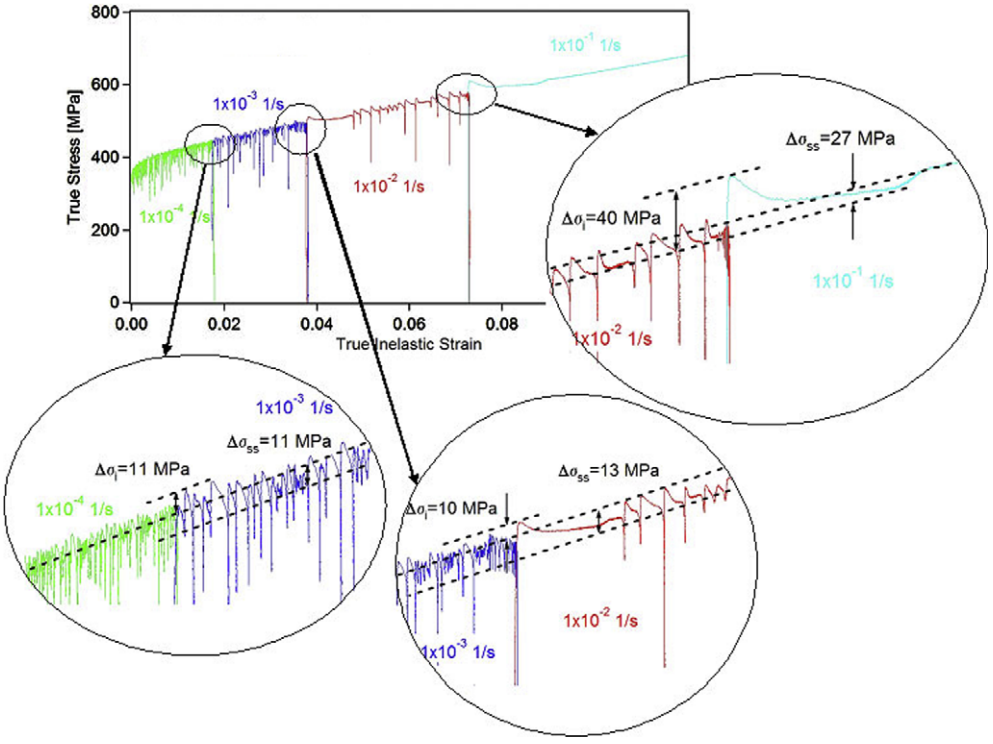

Figure 2. Results of a representative strain rate jump experiment.

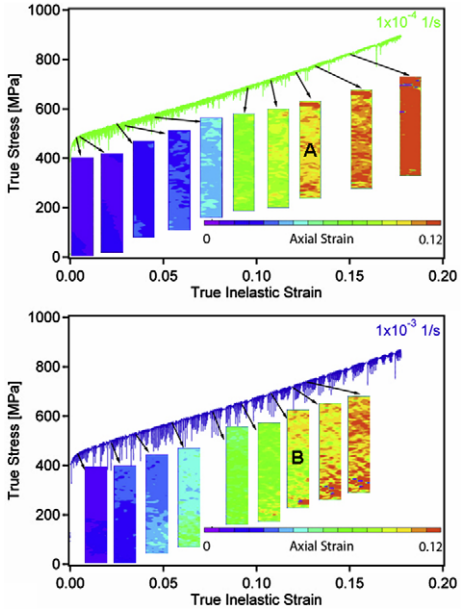

Figure 3. In situ DIC images demonstrating the evolution of local strain fields under monotonic tensile loading of Hadfield steel. The strain component along the axis of deformation is shown on the DIC images.

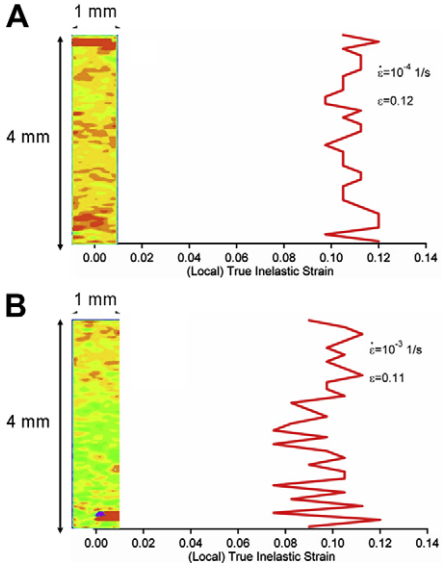

Figure 4. Comparison of strain localization in the NSRS range for strain rates of $1 \cdot 10^{-4} \frac{1}{s}$ and $1 \cdot 10^{-3} \frac{1}{s}$ at true inelastic strains of 0.12 and 0.11, respectively (Fig. 3). The strain data represents the variation along the center line of the gauge section.

present at these strain rates, as opposed to many other rate-sensitive materials [27–32,35].

The current study demonstrates that in situ DIC can serve as a means of macroscopically screening a phenomenon driven by atomistic mechanisms, such as DSA. The results of both mechanical experiments and DIC analysis show the existence of NSRS and strain localizations in Hadfield steel brought about by DSA, a major contributor to the rapid work hardening in this material.

The authors are grateful to Association of American Railroads, Pueblo, CO, USA, for supplying the material utilized in the work presented herein. The financial support of College of Engineering at Koc University,

Istanbul, Turkey and National Science Foundation program DMR-0803270 is appreciated.

[1] Y.N. Dastur, W.C. Leslie, Metall. Trans. A 12 (1981) 749.
[2] P.H. Adler, G.B. Olson, W.S. Owen, Metall. Trans. A 17 (1986) 1725.
[3] W.S. Owen, M. Grujicic, Acta Mater. 47 (1999) 111.
[4] Canadinc D., Ph.D. Thesis (2005), University of Illinois at Urbana-Champaign, USA.
[5] K.S. Raghavan, A.S. Sastri, M.J. Marcinkowski, Trans. TMS-AIME 245 (1969) 1569.
[6] I. Karaman, H. Sehitoglu, K. Gall, Y.I. Chumlyakov, H.J. Maier, Acta Mater. 48 (2000) 1345.
[7] I. Karaman, H. Sehitoglu, A.J. Beaudoin, Y.I. Chumlyakov, H.J. Maier, C.N. Tomé, Acta Mater. 48 (2000) 2031.
[8] I. Karaman, H. Sehitoglu, Y.I. Chumlyakov, H.J. Maier, I.V. Kireeva, Metall. Mater. Trans. A 32 (2001) 695.
[9] I. Karaman, H. Sehitoglu, Y.I. Chumlyakov, H.J. Maier, I.V. Kireeva, Scripta Mater. 44 (2001) 337.
[10] M.A. Shtremel, I.A. Kovalenko, Phys. Met. Metall. 63 (1987) 158.
[11] B.K. Zuidema, D.K. Subramanyam, W.C. Leslie, Metall. Trans. A 18 (1987) 1629.
[12] D. Canadinc, H. Sehitoglu, H.J. Maier, Y.I. Chumlyakov, Acta Mater. 53 (2005) 1831.
[13] D. Canadinc, H. Sehitoglu, H.J. Maier, Y.I. Chumlyakov, Int. J. Solids Struct. 44 (2007) 34.
[14] D. Canadinc, H. Sehitoglu, H.J. Maier, Mater. Sci. Eng. A 485 (2008) 258.
[15] A.H. Cottrell, B.A. Bilby, Proc. Phys. Soc. Lond. A 62 (1994) 49.
[16] A.H. Cottrell, M.A. Jawson, Proc. R. Soc. Lond. A 199 (1949) 104.
[17] A. Van Den Beukel, Phys. Stat. Sol. a30 (1975) 197.
[18] S.H. Van Den Brink, A. Van Den Beukel, P.G. McCormick, Phys. Stat. Sol. a30 (1975) 469.
[19] N. Louat, Scripta Metall. 15 (1981) 1167.
[20] P.G. McCormick, Acta Metall. 36 (1988) 3061.
[21] Y. Estrin, P.G. McCormick, Acta Metall. 39 (1991) 2977.
[22] P.G. McCormick, C.P. Ling, Acta Metall. Mater. 43 (1995) 1969.
[23] R.F. Hamilton, H. Sehitoglu, K. Aslantas, C. Efstathiou, H.J. Maier, Acta Mater. 56 (2008) 2231.
[24] B. Watrisse, A. Chrysochoos, J.-M. Muracciole, M. Némoz-Gaillard, Eur. J. Mech. A/Solids 20 (2001) 189–211.
[25] J. Kang, Y. Ososkov, J.D. Embury, D.S. Wilkinson, Scripta Mater. 56 (2007) 999.
[26] V. Tarigopula, O.S. Hopperstad, M. Langseth, A.H. Clausen, F. Hild, Int. J. Solids Struct. 45 (2008) 601.
[27] W. Tong, J. Mech. Phys. Solids 46 (1998) 2087.
[28] J. Kang, D.S. Wilkinson, J.D. Embury, M. Jain, A.J. Beaudoin, Scripta Mater. 53 (2005) 499.
[29] J. Kang, D.S. Wilkinson, M. Jain, J.D. Embury, A.J. Beaudoin, S. Kim, R. Mishira, A.K. Sachdev, Acta Mater. 54 (2006) 209.
[30] H. Halim, D.S. Wilkinson, M. Niewczas, Acta Mater. 55 (2007) 4151.
[31] N. Ranc, D. Wagner, Mater. Sci. Eng. A 394 (2005) 87.
[32] N. Ranc, D. Wagner, Mater. Sci. Eng. A 474 (2008) 188.
[33] W.A. Curtin, D.L. Olmsted, L.G. Hector Jr., Nat. Mater. 5 (2006) 875.
[34] M.A. Meyers, O. Vöhringer, V.A. Lubarda, Acta Mater. 49 (2001) 4025.
[35] W. Tong, N. Zhang, Trans. ASME 129 (2007) 332.

Please cite this article in press as: D. Canadinc et al., Scripta Mater. (2008), doi:10.1016/j.scriptamat.2008.07.027